

The 4MOST–Gaia Purely Astrometric Quasar Survey (4G-PAQS)

Jens-Kristian Krogager¹
 Karen M. Leighly²
 Johan Peter Uldall Fynbo^{3,4}
 Kasper Elm Heintz^{3,4}
 Sergei Balashev⁵
 Franz Erik Bauer^{6,7}
 Trystyn Berg^{5,8}
 Hyunseop Choi⁹
 Lise Bech Christensen^{3,4}
 Annalisa De Cia^{10,11}
 Sara Ellison¹²
 Stefan Geier^{13,14}
 Eilat Glikman¹⁵
 Neeraj Gupta¹⁶
 Christina Konstantopoulou¹⁰
 Daria Kosenko⁵
 Cédric Ledoux¹¹
 Sebastian López⁸
 Bo Milvang-Jensen^{3,4}
 Leah Morabito^{17,18}
 Palle Møller^{4,11}
 Pasquier Noterdaeme^{19,20}
 Max Pettini²¹
 Jason Xavier Prochaska^{22,23}
 Sandra Raimundo^{4,25,26}
 Johan Richard¹
 Raghunathan Srianand¹⁶
 Ksenia Telikova^{11,5}
 Donald Terndrup²⁷
 Todd M. Tripp²⁸
 Marianne Vestergaard^{4,24}
 Tayyaba Zafar²⁹

¹ CRAL, University Claude Bernard Lyon 1, ENS of Lyon, France

² Homer L. Dodge Department of Physics and Astronomy, The University of Oklahoma, USA

³ The Cosmic DAWN Center, Denmark

⁴ Niels Bohr Institute, University of Copenhagen, Denmark

⁵ Ioffe Institute, Saint Petersburg, Russia

⁶ Institute of Astrophysics and Centre for Astroengineering, Faculty of Physics, Pontifical Catholic University of Chile, Santiago, Chile

⁷ Millennium Institute of Astrophysics, Santiago, Chile

⁸ Department of Astronomy, University of Chile, Santiago, Chile

⁹ Department of Physics, University of Montreal, Canada

¹⁰ Department of Astronomy, University of Geneva, Switzerland

¹¹ ESO

¹² Department of Physics & Astronomy, University of Victoria, Canada

¹³ Gran Telescopio Canarias, La Palma, Spain

¹⁴ Canary Islands Institute of Astrophysics, Tenerife, Spain

¹⁵ Department of Physics, Middlebury College, USA

¹⁶ Inter-University Centre for Astronomy and Astrophysics, Pune, India

¹⁷ Centre for Extragalactic Astronomy, Department of Physics, Durham University, UK

¹⁸ Institute for Computational Cosmology, Department of Physics, Durham University, UK

¹⁹ Paris Institute of Astrophysics, France

²⁰ French-Chilean Laboratory for Astronomy, Santiago, Chile

²¹ Institute of Astronomy, University of Cambridge, UK

²² Department of Astronomy & Astrophysics, UCO/Lick Observatory, University of California, USA

²³ Kavli Institute for the Physics and Mathematics of the Universe, Kashiwa, Japan

²⁴ Dark Cosmology Centre, Niels Bohr Institute, University of Copenhagen, Denmark

²⁵ Department of Physics and Astronomy, University of California, Los Angeles, USA

²⁶ Department of Physics & Astronomy, University of Southampton, UK

²⁷ Department of Astronomy, The Ohio State University, USA

²⁸ Department of Astronomy, University of Massachusetts, USA

²⁹ Australian Astronomical Optics, Macquarie University, Australia

The 4MOST–Gaia Purely Astrometric Quasar Survey (4G-PAQS) will carry out the first large-scale, colour-independent quasar survey selected solely on the basis of astrometry from Gaia. Our main objective is to quantify the selection effects of current colour-selected samples. These colour-selected samples bias our view of the neutral gas and its chemical enrichment because of dust obscuration and reddening of optical colours. Moreover, the broad absorption-line outflows observed in quasars are under-represented by optical colour selection. 4G-PAQS will provide the first sample to overcome these challenges and will constrain the physical and chemical properties of gas in galaxies and quasars at cosmic noon.

Scientific context

Atomic and molecular gas in galaxies

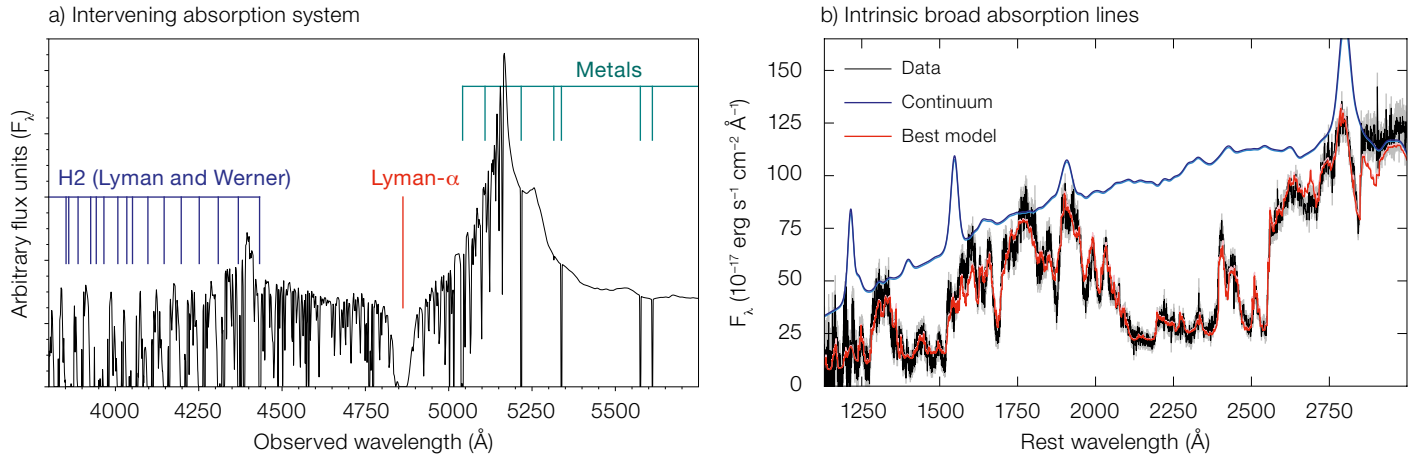
Studying HI absorption in spectra of luminous background sources such as quasars remains the best way to probe neutral hydrogen in individual galaxies beyond the local Universe ($z \geq 0.1$) until the advent of the Square Kilometre Array. Of particular interest for galaxy evolution studies are the so-called Damped Lyman- α Absorbers (DLAs; Wolfe, Gawiser & Prochaska, 2005), whose large HI column densities ($\log[N_{\text{HI}} \text{ cm}^{-2}] > 20.3$) arise in self-shielded, galactic environments. The neutral gas at even higher column densities ($\log[N_{\text{HI}} \text{ cm}^{-2}] \geq 21.5$) is sensitive to many physical processes, such as the formation of molecular hydrogen (H_2) and subsequently star formation (Bird et al., 2014; Noterdaeme et al., 2014).

Another important aspect of galaxy evolution is the buildup of metals over time and their redistribution in and around galaxies. Observations of DLAs offer a precise and model-independent way of measuring metallicities at high redshift through the numerous metal absorption lines observed in optical spectra of distant quasars (Prochaska et al., 2003; De Cia et al., 2018).

Owing to the cross-section selection of absorbers and the insensitivity of the Lyman- α transition to temperature, DLAs probe mostly the warm neutral medium ($T \sim 10^4 \text{ K}$). The cold neutral medium ($T \sim 100 \text{ K}$) is best traced by H_2 , found in only a few percent of the overall DLA population (Balashev & Noterdaeme, 2018). At high redshift, H_2 is directly detectable in optical spectra through Lyman and Werner bands in the rest-frame UV (900–1100 Å). The simulated quasar spectrum shown in Figure 1 (left panel) illustrates the molecular and atomic absorption features expected in our survey.

The impact of dust obscuration

If a significant amount of dust is present in the absorbing gas, the background quasar will appear fainter and redder than it is intrinsically. Quasars with dusty foreground systems are therefore more



likely to fall below the flux limit of optically selected spectroscopic surveys. Such quasar surveys will introduce a bias against dust-rich absorption systems (Pei, Fall & Bechtold, 1991). Since the amount of dust extinction scales with both metallicity and $N(\text{HI})$, the bias against dusty absorbers becomes a bias against high-metallicity and high- $N(\text{HI})$ systems (Pontzen & Pettini, 2009). Targeted searches for quasars reddened by foreground dusty absorbers have found many such cases (Krogager et al., 2015). The impact of dust bias in a purely flux-limited sample can be corrected using statistical modelling; however, current spectroscopic samples (such as SDSS) are also selected based on inhomogeneous optical and near-infrared colour criteria which are not easily corrected for.

Given the complex selection function of current quasar samples, the only way to make progress is by obtaining a reference sample of quasars and DLAs that is free from colour selection. Any foreground dust obscuration effects can then be corrected for in a statistical manner.

Quasar feedback at cosmic noon

Quasars may play an important role in shutting down star formation activity in galaxies and strong outflows are thought to be a key ingredient during quasar activity (Fabian et al., 2012). The broad absorption lines (BALs) observed in the rest-frame UV spectra of quasars are evidence for such powerful winds emerging from the central engine given their large,

blue-shifted velocities. These winds potentially contribute to the co-evolution of black holes and galaxies in a process known as quasar feedback (for example, Glikman et al., 2012 and references therein). Another important population of the overall quasar demographic is composed of intrinsically reddened quasars. These red quasars have moderate reddening ($E(B-V) \sim 0.25\text{--}1.5$ mag), such that their optical spectra are not fully dust obscured and still dominated by an AGN continuum and broad emission lines. Red quasars may represent a distinct evolutionary phase between a merger-driven starburst in a completely obscured AGN, and a normal, unreddened (i.e., blue) quasar (Urrutia, Lacy & Becker, 2008).

Large-scale optical surveys of quasars underestimate the fraction of both BAL quasars (BALQs) and red quasars as a result of the imposed optical-colour criteria (for example, Glikman et al., 2012; Fynbo et al., 2013). This is further supported by studies of radio-selected samples reporting larger numbers of reddened quasars (for example, White et al., 2003) and BALQs (Morabito et al., 2019). The colour-selection effects limit our understanding of the critical role that these objects play in the Universe.

Broad absorption lines and their link to red quasars

Low- and high-ionisation BALQs offer an array of absorption lines between 1020 and 3000 Å (rest-frame) that can be used to constrain the outflow properties (for

Figure 1. Noiseless mock 4MOST quasar spectrum featuring an intervening absorption system at $z = 3$ (left panel). The coloured marks indicate the absorption lines that allow us to quantify the chemical and physical properties of the absorbing gas: Lyman- α , H₂ lines and metal lines. The right-hand panel shows the best-fit synthetic BAL model to the SDSS spectrum of a FeLoBAL quasar allowing us to extract physical outflow parameters such as density, ionisation parameter and outflow velocity (Choi et al., 2020).

example, Leighly et al., 2018). The BAL outflow velocity is observed to correlate with luminosity and because of the strong dependence of outflow energy on velocity (outflow kinetic luminosity, $L_{\text{kin}} \propto v^3$), luminous quasars are potentially the strongest sources of feedback among BALQs.

FeLoBAL quasars — a subset of low-ionisation BALQs — have a myriad of absorption lines from Fe⁺ in their near-UV spectra (see Figure 1, right panel), and therefore they can be studied over a wide redshift range from 0.8 to 4. This range includes the cosmic noon, where feedback may have been especially impactful. Sixty percent of red quasars show BALs in their spectra, nearly all of which are low-ionisation BALs or FeLoBALs.

Specific scientific goals

The goal of 4G-PAQS is to obtain a colour-unbiased reference sample of quasars and their foreground absorbers. With this core sample of quasars, we will address the scientific goals set out below.

The unbiased cosmic mass density of metals from $2 < z < 3$

It has been shown that DLAs trace a significant fraction of metals over cosmic time, reaching $\sim 100\%$ of the inferred metal mass, $\Omega_{\text{Met, TOT}}$, at $z = 4$ (Péroux & Howk, 2020). However, this fraction is observed to decrease with decreasing redshift, based on optically selected samples. The colour-selection criteria of current optical quasar samples introduce a redshift dependence on the dust bias (Krogager et al., 2019) that directly affects the measured cosmic mass density of metals, Ω_{Met} . While Ω_{Met} at $z = 3$ may be underestimated by a factor of around two, this increases to a factor of around three at $z = 2$. Such a redshift-dependent bias would counteract the observed decrease in $\Omega_{\text{Met}} / \Omega_{\text{Met, TOT}}$. Our aim with this survey is to constrain Ω_{Met} as a function of redshift from an unbiased sample of nearly 2000 high-redshift DLAs.

The unbiased absorption cross-section of HI and H₂ at $z > 2$

Current numerical simulations are still unable to reproduce the observed redshift evolution of the HI absorption cross-section as inferred by the so-called line incidence, dn/dz (Bird et al., 2014; Hassan et al., 2020). If a dust bias is present in current observations, it is important to correct for this before drawing conclusions about feedback mechanisms in simulations. Moreover, simulations are only recently starting to resolve the cold (H₂) and warm (HI) neutral media in cosmological volumes (for example, Nickerson, Teyssier & Rosdahl, 2019; Feldmann et al., 2022). Hence, constraining the dn/dz of H₂ and HI in an unbiased sample will provide the first comparison to these new simulations.

What is the true number of BALQs?

Another core goal of 4G-PAQS is to quantify the unbiased, intrinsic fraction of BALQs and the physical conditions of the outflowing material over the redshift range $0.8 < z < 4$. The fraction of BALQs depends on the sample selection: Hewett & Foltz (2003) infer a fraction of 20% in

optically selected samples, but it may be as large as 40%, depending on the source luminosity (Bruni et al., 2019). There is further observational evidence that BALQs are 3.5 times as common at $z = 4$ as at $z = 2$ (Allen et al., 2011). This may be evidence that black hole feedback evolves, something that may be important for constraining feedback models, if the fraction of quasars that have BALs reflects the global covering fraction of the outflowing gas.

What are the gas properties of BAL outflows?

We aim to characterise the physical properties of the outflow in each quasar to obtain better insight into the potential interrelation between individual quasar subtypes (low-ionisation versus high-ionisation BALs and red quasars). This may provide a basis for understanding the link, if present, between each quasar subtype and different galaxy merger stages. We will use our novel spectral synthesis software SimBAL (Leighly et al., 2018) on the sample of BALQs to trace the outflow properties and feedback over cosmic time. An example of the spectral fitting is presented in Figure 1. Depending on the absorption lines present, we can obtain excellent constraints on the physical properties of the winds (ionisation parameter, density) which in turn yield measurements of the outflow properties (location, mass outflow rate, kinetic luminosity; Choi et al., 2020).

What is the true number of red quasars?

We aim to constrain black hole masses and accretion rates and determine the properties and representative fractions of the overall quasar population (red, blue and BAL sub-types). Intrinsically reddened quasars make up $\sim 20\text{--}30\%$ of quasars (Glikman et al., 2012). However, current representative samples are small (~ 150 objects), which makes it difficult to study any redshift evolution of the red quasar population. Since the red quasar phenomenon may be linked to an evolutionary phase with higher accretion rates (Kim et al., 2015), measuring the black

hole masses and accretion rates in a representative, unbiased sample will be crucial for quantifying any redshift evolution. If the red quasar phenomenon is an evolutionary phase, then determining their fraction as a function of redshift would constrain the duration of that phase.

Identifying rare quasars

Lastly, our purely astrometric selection with no assumptions about spectral shape will have significant potential to discover outlying and rare objects that may be overlooked otherwise (Hall et al., 2002; Geier et al., 2019). Our survey aims to identify rare quasars in a representative sample and to quantify the prevalence of such rare objects.

Target selection and survey area

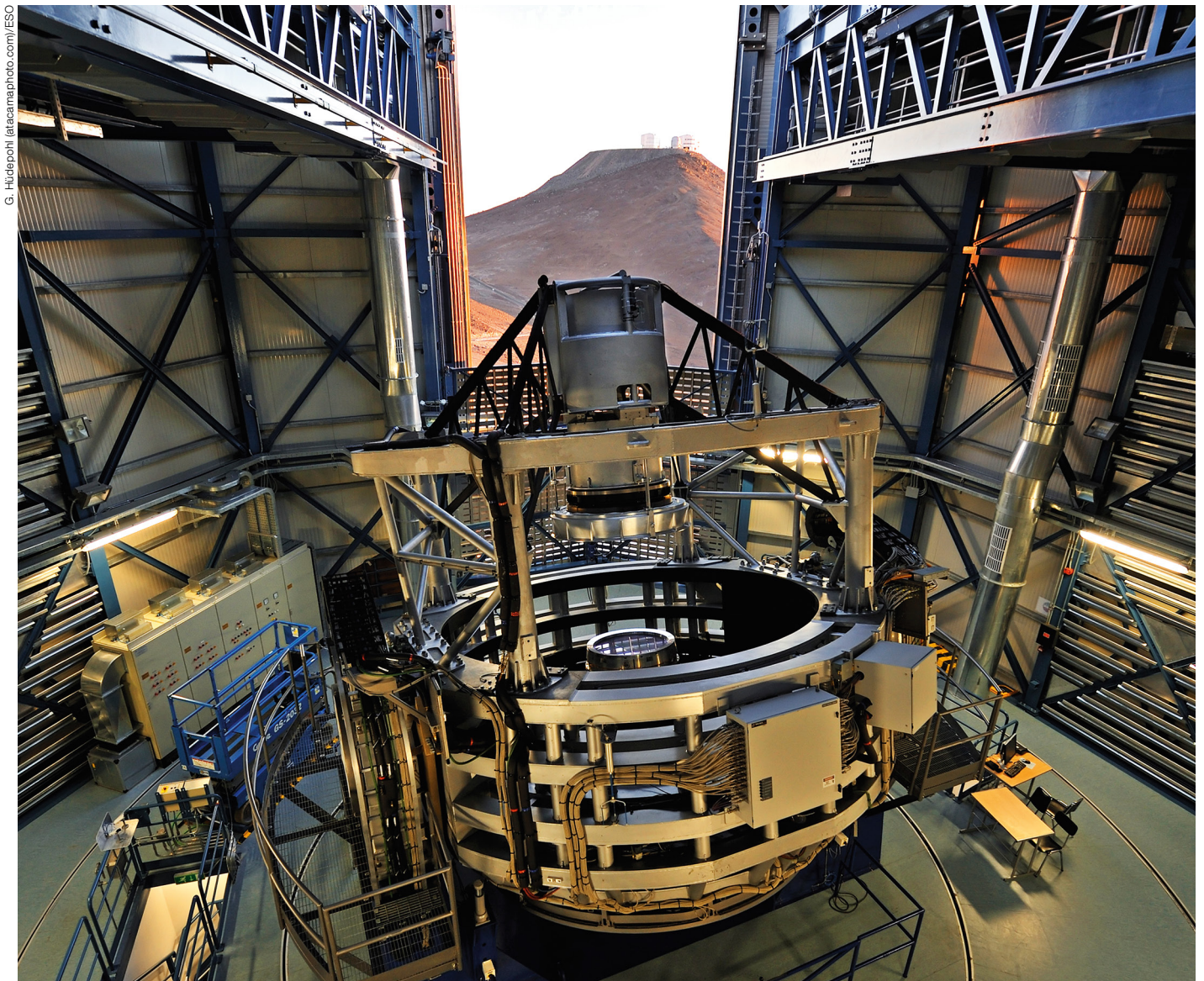
Candidate quasars for 4G-PAQS are selected purely on the basis that quasars are stationary sources on the sky (Heintz et al., 2018). We select sources from the Gaia catalog with proper motions and parallaxes consistent with zero at the 2σ level down to a limit of $G < 20.5$ mag. The completeness of our survey is therefore limited only by the fibre allocation efficiency (up to $\sim 80\%$). However, since the fibre allocation does not depend on the colour of the targets, this lower completeness will not introduce any selection bias.

Since the number of stationary sources in the Gaia catalogue increases drastically when observing close to the Galactic plane, we have limited our survey area to high Galactic latitudes, $b < -60$ deg. Based on a pilot study carried out at the North Galactic Pole (Heintz et al., 2020), we have estimated the stellar contamination to be around 40% over the entire survey area.

In total, 4G-PAQS will obtain a colour-unbiased sample of $\sim 100\,000$ quasars with no prior selection on the basis of redshift or spectral shape. Our sample will therefore be purely flux limited. To reach the above scientific goals, we will obtain spectra with a signal to noise ratio of at least 5 \AA^{-1} over $7700\text{--}8500 \text{ \AA}$.

References

- Allen, J. T. et al. 2011, MNRAS, 410, 860
Balashev, S. A. & Noterdaeme, P. 2018, MNRAS, 478, 7
Bird, S. et al. 2014, MNRAS, 445, 2313
Bruni, G. et al. 2019, A&A, 630, A111
Choi, H. et al. 2020, ApJ, 891, 53
De Cia, A. et al. 2018, A&A, 611, A76
Fabian, A. C. 2012, ARA&A, 50, 455
Feldmann, R. et al. 2022, arXiv:2205.15325
Fynbo, J. P. U. et al. 2013, ApJS, 204, 6
Geier, S. J. et al. 2019, A&A, 625, L9
Glikman, E. et al. 2012, ApJ, 757, 51
Hall, P. B. et al. 2002, ApJS, 141, 267
Hassan, S. et al. 2020, MNRAS, 492, 2835
Heintz, K. E. et al. 2018, A&A, 615, L8
Heintz, K. E. et al. 2020, A&A, 644, A17
Hewett, P. C. & Foltz, C. B. 2003, AJ, 125, 1784
Kim, D. et al. 2015, ApJ, 812, 66
Krogager, J.-K. et al. 2015, ApJS, 217, 5
Krogager, J.-K. et al. 2019, MNRAS, 486, 4377
Leighly, K. M. et al. 2018, ApJ, 866, 7
Morabito, L. K. et al. 2019, A&A, 622, A15
Nickerson, S., Teyssier, R. & Rosdahl, J. 2019, MNRAS, 484, 1238
Noterdaeme, P. et al. 2014, A&A, 566, A24
Pei, Y. C., Fall, S. M. & Bechtold, J. 1991, ApJ, 378, 6
Péroux, C. & Howk, J. C. 2020, ARA&A, 58, 363
Pontzen, A. & Pettini, M. 2009, MNRAS, 393, 557
Prochaska, J. X. et al. 2003, ApJ, 595, L9
Urrutia, T., Lacy, M. & Becker, R. H. 2008, ApJ, 674, 80
White, R. L. et al. 2003, AJ, 126, 706
Wolfe, A. M., Gawiser, E. & Prochaska, J. X. 2005, ARA&A, 43, 861



This spectacular view of the VISTA telescope was taken from the roof of the building during the opening of the enclosure at sunset. The VLT is visible on the neighbouring mountain. VISTA is the largest

survey telescope in the world and it is dedicated to mapping the sky at near-infrared wavelengths. Its primary mirror is 4.1 metres in diameter and is the most highly curved of its size. The extremely high

curvature reduces the focal length, making the structure of the telescope extremely compact. VISTA can map large areas of the sky quickly and deeply.